International Journal of Marine Science and Technology, vol. 2, no. 1, pp. 23–30, 2026 e-ISSN: 3093-3609
https://doi.org/10.65154/ijmst.22 https://i-jmst.vimaru.edu.vn

The Effects of a Triangular Floating Platform and Dual Surface-piercing Thin Barriers over a Sloped Bottom on Wave Reflection

Chang Tran Thi*

Abstract: This study analytically investigates the wave reflection from a triangular floating platform in conbination with dual surface-piercing thin barriers over a sloped bottom using the eigenfunction matching method (EMM). The problem is formulated with linear water wave theory; eigenfunction expansions describe wave interactions across regions with varying bathymetry and boundaries. By imposing continuity of velocity potential and pressure at interfaces, a numerically solvable system is established. Reflection coefficients are analyzed with varying platform, barrier, and seabed parameters. Results show that barrier configuration and seabed slope significantly affect the reflected wave. The findings inform the design of structures for wave energy dissipation, platform protection, and nearshore barriers.

Keywords: Eigenfunction matching method, floating platform, reflected waves, sloped bottom, thin barriers.

1. INTRODUCTION

The interaction of linear and nonlinear waves with floating platforms and coastal or offshore barriers has long been a central topic in marine hydrodynamics, owing to its direct relevance to coastal protection, offshore engineering, and renewable energy harvesting. Accurate prediction of water wave reflection and scattering in the presence of complex structural configurations is essential for designing and assessing the performance of floating breakwaters, floating energy devices, and multi-functional offshore platforms.

Previous research has explored the propagation of water waves by various types of single thin barriers, including surface-piercing barriers, bottom-standing barriers, and barriers with gaps, placed over a flat bottom [1]. In the research of Losada [2-4], the scattering of oblique incidence waves by multiple thin barriers was investigated. The porosities of thin barriers are then studied in the applications of enhancing wave energy dissipation [5-8].

Floating platforms (FPs) also provide practical uses, as their surfaces can function as roads, mooring points, or fishing piers [9]. Recently, Mondal and Alam [10] examined how various parameters affect wave reflection and transmission in arrays of identical rectangular FPs placed over a heterogeneous seabed, considering both infinite and semi-infinite fluid domains. The combination of floating platforms with thin barriers enables tuning the system response through barrier design parameters, making it suitable for deep water areas and sensitive utility installations, allowing more effective wave energy dissipation and enhanced protection against wave loads compared to conventional floating structures alone. One approach involves installing vertical tensioned barriers or submerged dual barriers in front of or enclosing a compliant floating platform [11], which supports utility systems like solar panels. These barriers help reduce wave-induced platform motion and improve stability, with performance influenced by barrier length, porosity, and hydroelastic properties [12]. Research on floating platforms combined with dual surface-piercing thin barriers has predominantly focused on prototype-scale configurations and specialized applications. These configurations use thin, vertical barriers extending above the water surface to shield platforms from incoming waves [13]. The effects of these configurations have been investigated in terms of mitigating platform motions induced by incident wave action [14].

Among various analytical and numerical techniques, the eigenfunction matching method (EMM) has proven to be a highly effective semi-analytical approach in solving wave–structure interaction problems, particularly in cases involving piecewise-constant or regularly varying boundaries. In the earlier studies, the EMM was soon applied to investigate the problems of water waves

Manuscript received October 31, 2025; received in revised form December 10, 2025; accepted December 26, 2025; available online March 30, 2026.

Chang Tran Thi is with the Department of Maritime Safety Engineering, Faculty of Civil Engineering, Vietnam Maritime University, Haiphong, Vietnam (e-mail: changtt.ctt@vimaru.edu.vn).
* Corresponding author.

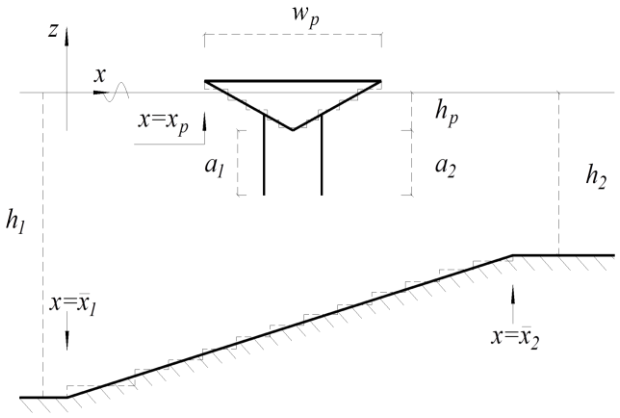

Fig. 1. Sketch of problems.

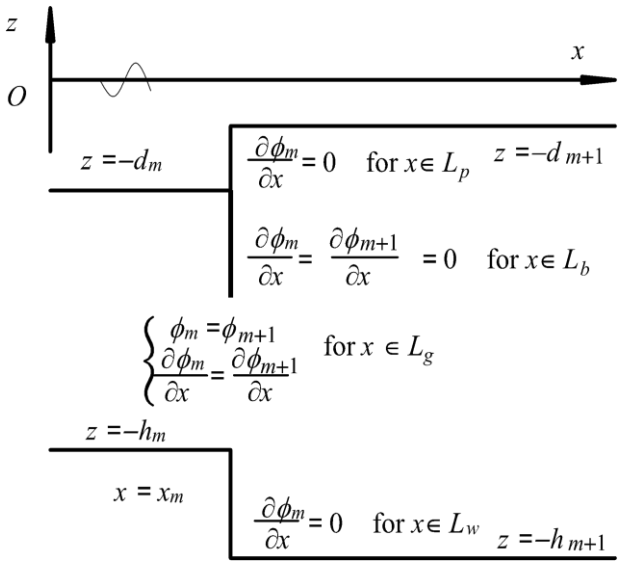

Fig. 2. Definition of a floating platform with a barrier over stepped bottom.

propagated over simple to more complex infinite steps [15,16]. In the research on the propagation of waves over an undulated bottom, the EMM deals with the concepts of a series of continuous flat steps [17]. Besides, the more complex interactions of water waves with thin rigid barriers [18-20] and slotted barriers [21] over undulated bottom are recently investigated by means of applying EMM.

There have been numerous studies on the water waves interactions with thin barriers, FPs, and undulated seabed. However, the researches on the effects of thin barriers which attached to the FP over sloped bottom topography in the enhancing waves propagations are rare. This study aims to conduct an analytic examination of the EMM in the context of wave reflected by a single triangular FP and multiple thin barriers over sloped bottom. By formulating the governing velocity potential in eigenfunction expansions valid for each fluid subdomain, the method enables systematic enforcement of boundary and continuity conditions at structural and bottom interfaces. Furthermore, detailed parametric studies illustrate the respective and combined effects of floating platform geometry, quantity and spacing of barriers, and seabed undulation. The results contribute significantly to guidelines in optimizing coastal defense systems and floating platform layouts in environments where seabed undulations and wave–structure interference effects play a significant role.

The organization of this paper is as follows. Section 2 develops the mathematical modeling framework for water wave phenomena and introduces the formulation of the eigenfunction matching method (EMM). Section 3 examines various validation cases to demonstrate the effectiveness of the proposed EMM approach. Detailed discussion on wave reflection involving a triangular floating platform with dual thin barriers along a sloped seabed is provided in Section 4. Finally, Section 5 offers overarching conclusions. The research findings advance practical applications in coastal engineering, including the design and analysis of breakwaters, seawalls, and other protective structures, as well as enriches insight into key physical processes such as wave propagation, refraction, diffraction, and reflection.

2. MATHEMATICAL MODEL

The behavior of surface waves, considering parameters such as angular frequency σ, wave amplitude $\bar{a}$, angle of approaching wave γ, with wavelength λ , interacting with a sloped bottom, containing thin barriers, is analyzed using a two-dimensional coordinate system (x, z). In this context, the vertical direction is designated as the z-axis is chosen upward, while the horizontal aligns with the x-axis. The general investigating problem of water waves interacting with the single triangular FP with dual thin barriers over a sloped bottom is demonstrated in Figure 1. The wave amplitude is presumed to be sufficiently small to justify the use of linear wave theory, where wave shape is sinusoidal, kinematics and dynamic pressure vary harmonically, and dispersion relations and response functions (for example: reflection coefficient $|R|$, or transmission coefficient $|T|$) are straightforward and analytically tractable. The wave motion is assumed to be time-harmonic, with its temporal behavior described by $e^{-\mathbf{i}\sigma t}$, where σ is defined by $2\pi/T$ denotes the angular frequency based on wave period T. Besides, t and $\mathbf{i}$ respectively denote the time variable and imaginary unit. For the sake of simplicity in the modelling of the topography, thin barriers and floating platform, the seabed could be segmented into a sequence of M shelves in the interval of $x_{m-1} \le x \le x_m$ for $m = 1, 2, \ldots, M$ with a specific water depth h_M . Additionally, certain standard assumptions regarding boundary conditions and wave properties are adopted. The i-th surface-piercing barrier is positioned at a specified location $x = v_i$, where its submerged portion has a length equal to a_i. Likewise, the i-th bottom-standing barrier is positioned at designated point $x = w_i$, and has a length of b_i. In the case that there is only a single surface-piercing or bottom-standing barriers, $a = a_i, v = v_i, b = b_i$ or $w = w_i$, the notation reduces accordingly for clarity throughout this paper.

Considering a single step that separates the shelves as illustrated in Figure 2, the vertical intervals of the barrier

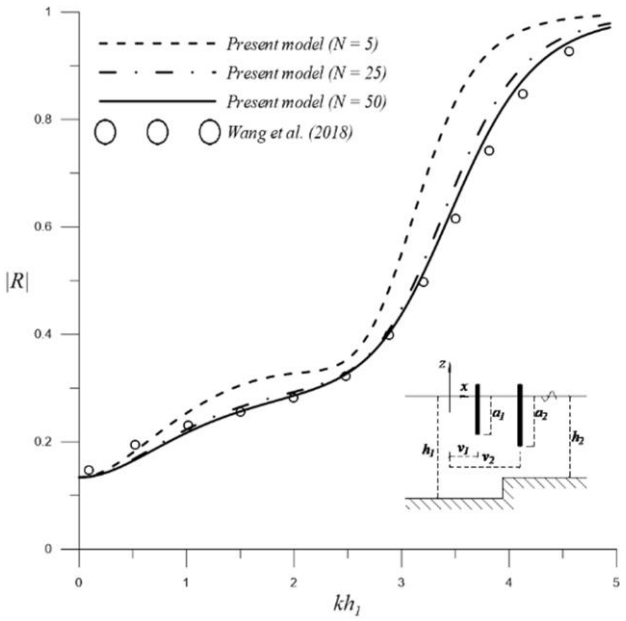

Fig. 3. Variations of $|R|$ against dimensionless parameter kh_1 for the case of parallel surface-piercing barriers over the stepped bottom, where $N = 5, 25, \text{and } 50$.

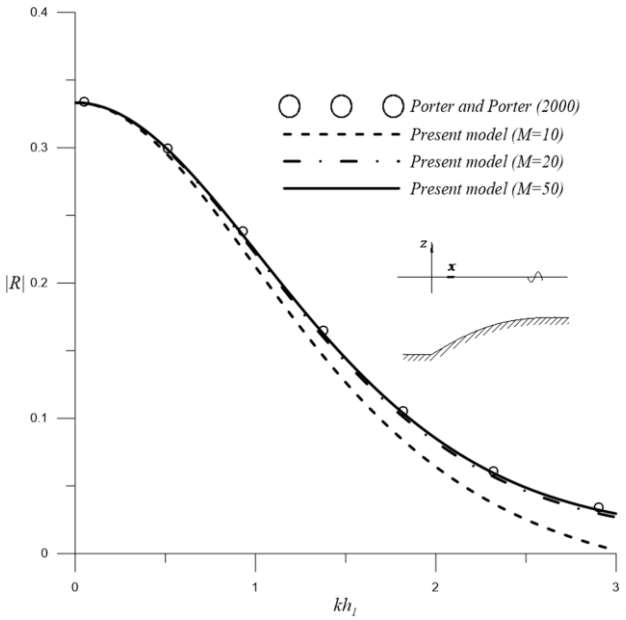

Fig. 4. Variations of $|R|$ against dimensionless parameter kh_1 for the case uneven bottom topography, where M = 10, 20, and 50.

and the gap are denoted by $L_b \; and \; L_g$ accordingly, while those of the platform and the bottom are also defined by L_p and L_w. If there is no barrier, L_b is omitted. For the m -th shelf within the interspace $x_{m-1} \le x \le x_m$ for $m = 1, 2, \dots, M$, the fluid velocity u_m is represented and can be formulated by

$$u_m = \nabla \phi_m \tag{1}$$

where the two-dimensional operator $\nabla = (\partial/\partial x, \partial/\partial z)$ specifies the coordinate system (x, z), while ϕ_m represents the velocity potential.

As a result, in order to meet the Laplace equation within the fluid domain

$$\nabla^2 \phi_m = 0 \tag{2}$$

The boundary conditions of kinematic, dynamic, and bottom can be found in the research of Tran, Chang and Tsai [18]

The velocity potential ϕ_m is the solution on the shelf. The wall boundary condition is considered only for the deeper shelf. To ensure the continuation and smooth transitions between the m-th and the $m+1$-th shelf, there are requirements for the connection conditions of velocity potentials ϕ_m and ϕ_{m+1}

$$\phi_m = \phi_{m+1} \text{ for } x \in L_g \tag{3}$$

$$\frac{\partial \phi_m}{\partial x} = \frac{\partial \phi_{m+1}}{\partial x} = 0 \text{ for } x \in L_b \tag{4}$$

$$\frac{\partial \phi_m}{\partial x} = \frac{\partial \phi_{m+1}}{\partial x} \text{ for } x \in L_g \tag{5}$$

$$\frac{\partial \phi}{\partial x} = 0 \text{ for } x \in L_w \text{ and } x \in L_p \tag{6}$$

Intending to make the solution uniquely solvable, it is necessary to have the following far-field conditions for the surface elevation

$$\eta = \bar{a}\left(e^{\mathbf{i}\hat{k}_{1,0}x} + K_R e^{\mathbf{i}\theta_R} e^{-\mathbf{i}\hat{k}_{1,0}x}\right) e^{-\mathbf{i}k_{1,0}y} \quad \text{as } x \to -\infty \tag{7}$$

and

$$\eta = \bar{a} K_T e^{\mathbf{i}\theta_T} e^{\mathbf{i}\hat{k}_{M,0}x} e^{\mathbf{i}k_y y} \quad \text{as } x \to \infty \tag{8}$$

where the numerical values assigned to the reflection and transmission coefficients are defined by components K_R, K_T, θ_R and θ_T, and correspondingly specified by $K_R e^{\mathbf{i}\theta_R}$ and $K_T e^{\mathbf{i}\theta_T}$.

In Eqs. (7) and (8), $\hat{k}_{M,0}, k_y$, and $\hat{k}_{1,0}$ are real-valued wavenumbers expressed by

$$\hat{k}_{m,n} = \sqrt{k_{m,n}^2 - k_y^2} \tag{9}$$

and

$$-\mathbf{i}\sigma\eta_m + \frac{\partial \phi_m}{\partial z} = 0 \tag{10}$$

$$k_y = k_{1,0} \sin\gamma \tag{11}$$

Additionally, the wavenumber in the case of a FP over a shelf ($d_m > 0$) is alternatively defined as

$$k_{m,n} = \frac{\mathbf{i}n\pi}{h_m - d_m} \tag{12}$$

where $k_{1,0} = 2\pi/\lambda > 0$ and $k_{m,0} > 0$ are the propagation number of wave which can be calculated via the dispersion relation

$$\frac{\sigma^2}{g} = k_{m,0} \tanh k_{m,0} h_m \tag{13}$$

The property of the dispersion relation for the shallow-water and deep-water conditions was previously investigated [22,23], where

$$\begin{cases} h < \lambda/20 & \text{for shallow water} \\ h > \lambda/2 & \text{for deep water} \end{cases} \tag{14}$$

In Eq. (12), the indices vary as $m = 1, 2, \dots, M$, and $n = 0, 1, 2, \dots$ Moreover, also in the Eq. (12), $k_{m,n}$ with $n > 0$ are presented as

$$k_{m,n} = \mathbf{i}\kappa_{m,n} \tag{15}$$

where $\kappa_{m,n}$ indicates the n-th ordered positive root determined by the dispersion relation

$$\frac{\sigma^2}{g} = -\kappa_{m,n} \tan \kappa_{m,n} h_m \tag{16}$$

$$k_{m,0} \tanh k_{m,0} h_m = K \text{ for } m = 1, 2, \dots, M \tag{17}$$

According to linear water wave theory, the velocity potential corresponding to the m -th shelf can be represented as follows

$$\phi_m(x, z) =$$

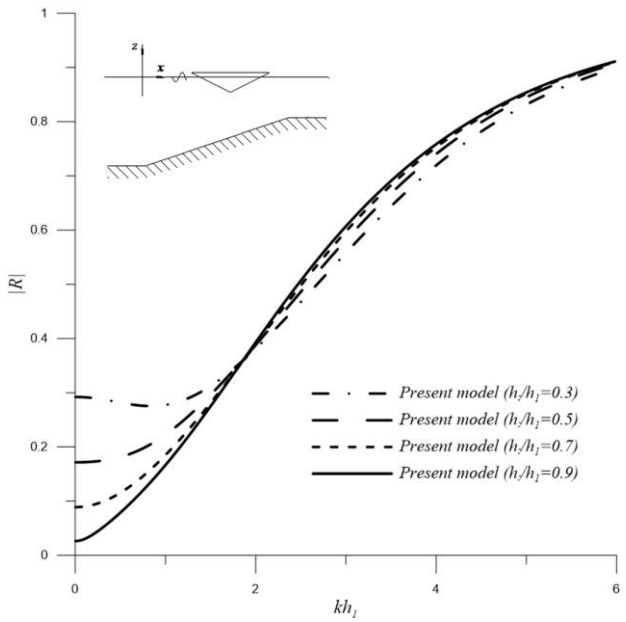

a) Reflection coefficient.

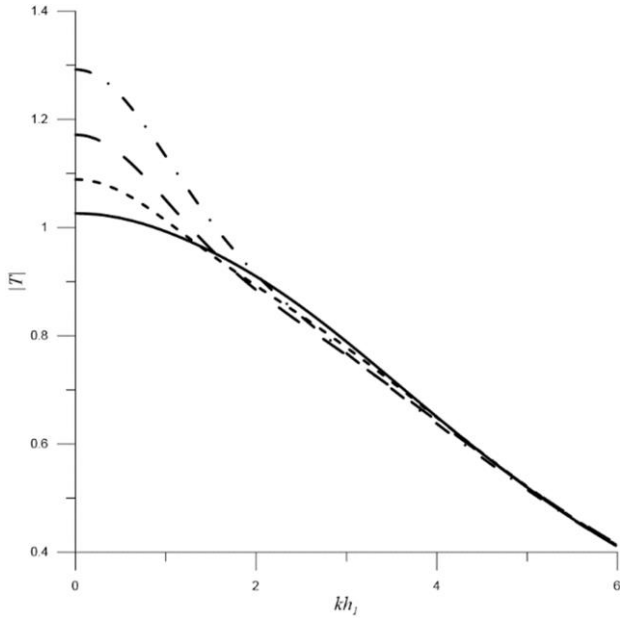

b) Transmission coefficient.

Fig. 5. Variations of a) $|R|$ and b) $|T|$ against dimensionless parameter kh_1 with values of bottom depth h_2/h_1=0.3; 0.5; 0.7; and 0.9.

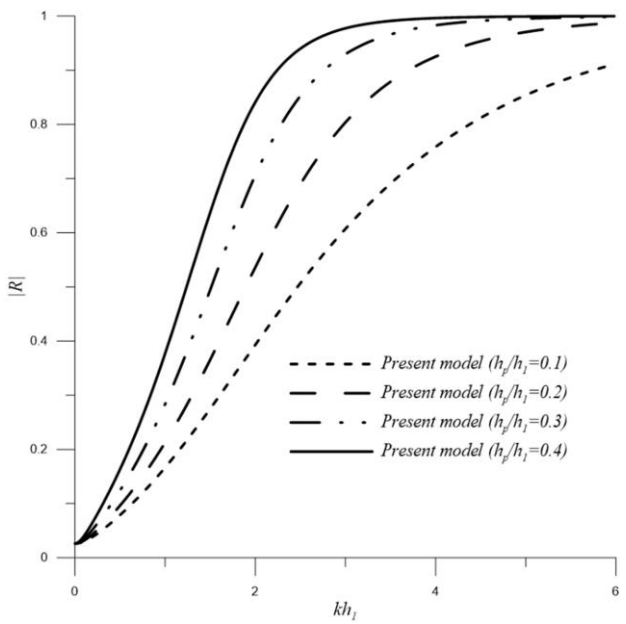

a) Reflection coefficient.

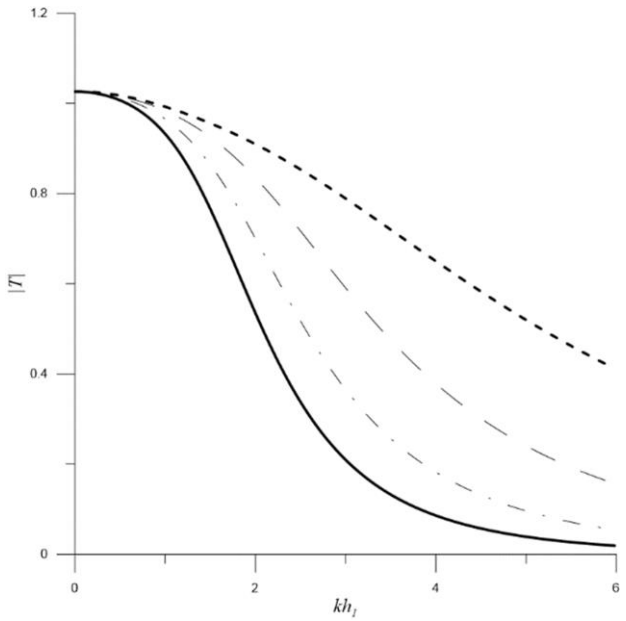

b) Transmission coefficient.

Fig. 6. Variations of a) $|R|$ and b) $|T|$ against dimensionless parameter kh_1 with values of platform depth h_p/h_1=0.1; 0.2; 0.3, *and* 0.4.

$$\sum_{n=0}^{N}\left(A_{m,n}\xi_{m,n}^{(1)}(x)+B_{m,n}\xi_{m,n}^{(2)}(x)\right)\zeta_{m,n}(z)e^{\mathrm{i}k_y y} \quad \text{for } m=1,2,\dots,M \tag{18}$$

$$\phi_{m+1}=\left(A_{m+1,n}\xi_{m+1,n}^{(1)}+B_{m+1,n}\xi_{m+1,n}^{(2)}\right)\zeta_{m+1,n} \tag{19}$$

where unknown coefficients $A_{m,n}$ and $B_{m,n}$ need to be solved since *m=1, 2, ..., M*. The factor *N* in Eq.(18) is assumed to be the evanescent mode number. By isolating the variables, the eigenfunctions in Eq.(18) can be defined as

$$\zeta_{m,n}(z)=\cosh k_{m,n}h_m+z \tag{20}$$

$$\xi_{m,n}^{(1)}(x)=\begin{cases}e^{\mathrm{i}\hat{k}_{m,n}(x-\bar{x}_{m-1})} & \hat{k}_{m,n}\neq 0\\ 1 & \hat{k}_{m,n}=0\end{cases} \tag{21}$$

and

$$\xi_{m,n}^{(2)}(x)=\begin{cases}e^{-\mathrm{i}\hat{k}_{m,n}(x-\bar{x}_m)} & \hat{k}_{m,n}\neq 0\\ x & \hat{k}_{m,n}=0\end{cases} \tag{22}$$

with

$$\begin{cases}\bar{x}_m=x_m\\ \bar{x}_0=\bar{x}_M=0\end{cases} \text{ for } m=1,2,\dots,M-1 \tag{23}$$

An examination of Eqs. (9)-(23) reveals that the solution satisfies the dynamic boundary conditions and bottom boundary conditions. By utilizing Eqs. (3)-(8), the values for the unknown coefficients $A_{m,n}$ and $B_{m,n}$ can be determined.

Subsequently, the eigenfunction matching method is employed to establish mass conservation as described in Eqs. (3)-(6)

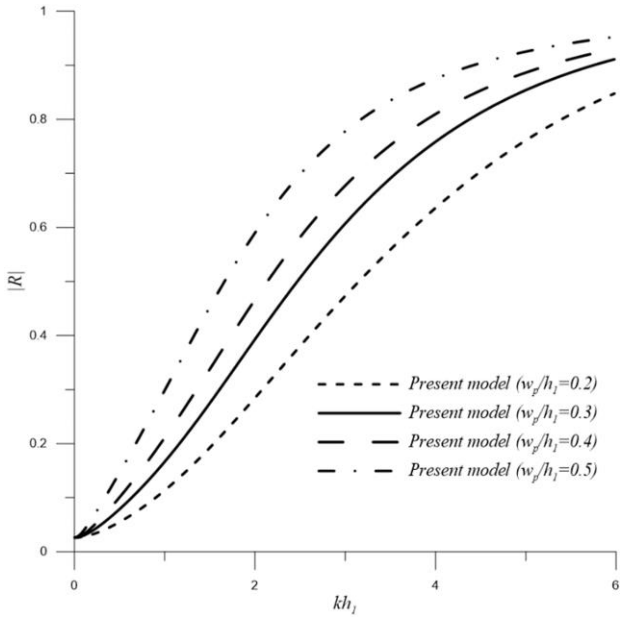

a) Reflection coefficient.

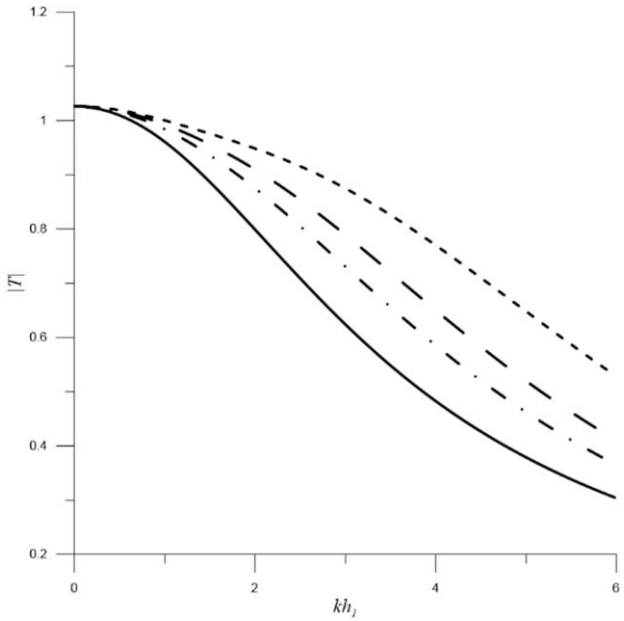

b) Transmission coefficient.

Fig. 7. Variations of a) $|R|$ and b) $|T|$ against dimensionless parameter kh_1 with values of platform width w_p/h_1=0.2; 0.3; 0.4; and 0.5.

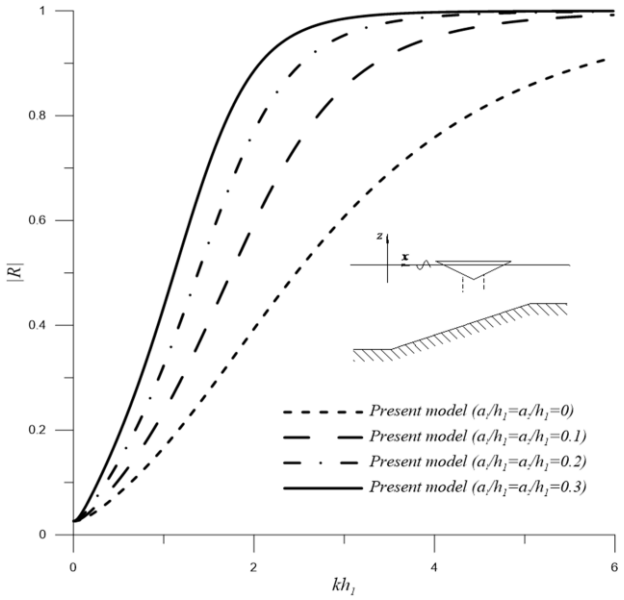

a) Reflection coefficient.

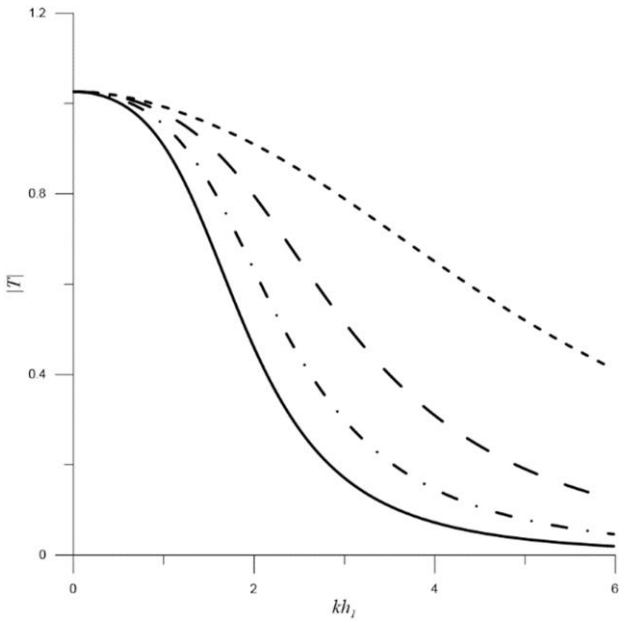

b) Transmission coefficient.

Fig. 8. Variations of a) $|R|$ and b) $|T|$ against dimensionless parameter kh_1 with values of barrier length $a_1/h_1 = a_2/h_1 = a_i/h_1 = 0;\ 0.1;\ 0.2;$ and 0.3.

$$\langle \frac{\partial \phi_m}{\partial x} \Big| \zeta_{m,l}^{larger} \rangle = \langle \frac{\partial \phi_{m+1}}{\partial x} \Big| \zeta_{m,l}^{larger} \rangle \quad \text{for } l = 0,1,2,\dots,N \tag{24}$$

where the smaller products of two depth eigenfunctions would be described as

$$\langle P_1 | P_2 \rangle = \int_{-h}^{0} P_1(z) P_2(x) dz \tag{25}$$

Both functions P_1 and P_2 denote the depth-dependent eigenfunctions of $\zeta_{m,n}$, which associated with arbitrary integers m and n. Moreover, h represents the water depth in terms of the corresponding eigenfunction P_1.

The momentum conservation law, together with the condition of the barrier, is summarized as follows

$$\langle \zeta_{m,l}^{smaller} | F \rangle = 0 \quad l = 0,1,\dots,N \tag{26}$$

where

$$F(\mathrm{z}) = \begin{cases} \phi_m(x_m) - \phi_{m+1}(x_m) & \text{for } x \in L_g \\ \frac{\partial \phi_m}{\partial x}\Big|_{x=x_m} & \text{for } x \in L_b \end{cases} \tag{27}$$

and

$$\langle \zeta_{m,l}^{smaller} | F \rangle = 0 \quad \text{for } l = 0,1,\dots,N \tag{28}$$

Eq.(26) can be rewritten as

$$\langle \zeta_{m,l}^{smaller} | \phi_m(x_m) \rangle = \langle \zeta_{m,l}^{smaller} | \phi_{m+1}(x_m) \rangle + \langle F | \zeta_{m,l}^{smaller} \rangle \quad \text{for } l = 0,1,2,\dots,N, \tag{29}$$

with

$$F = \left(\phi_m(x_m) - \phi_{m+1}(x_m)\right) - \frac{\partial \phi_m}{\partial x}\Big|_{x=x_m} \quad (30)$$
$$\text{for } x \in L_b$$

Subjected to the boundary conditions and the far-field conditions as defined in Eqs. (7) and (8), the formulate of the velocity potential far-field solutions can be written as

$$\phi_1 = \frac{\mathbf{i}\bar{a}g}{\sigma}\frac{\cosh k_{1,0}(h_1+z)}{\cosh k_{1,0}h_1}\left(e^{\mathbf{i}\hat{k}_{1,0}x} + K_R e^{\mathbf{i}\theta_R}e^{-\mathbf{i}\hat{k}_{1,0}x}\right)e^{\mathbf{i}k_y y}$$
$$\text{as } x \to -\infty \quad (31)$$

and

$$\phi_M = -\frac{\mathbf{i}\bar{a}g}{\sigma}\frac{\cosh k_{M,0}(h_M+z)}{\cosh k_{M,0}h_M}\left(K_T e^{\mathbf{i}\theta_T}e^{\mathbf{i}\hat{k}_{M,0}x}\right)e^{\mathbf{i}k_y y}$$
$$\text{as } x \to \infty \quad (32)$$

Combining Eqs. (31) and (32) into Eq.(18), the resulting equations are as follows

$$B_{1,0}e^{\mathbf{i}\hat{k}_{m,n}x} = -\frac{\mathbf{i}\bar{a}K_R e^{i\theta_R}}{\sigma}\frac{1}{\cosh k_{1,0}h_1} \quad (33)$$

$$A_{1,0} = -\frac{\mathbf{i}\bar{a}g}{\sigma}\frac{1}{\cosh k_{1,0}h_1} \quad (34)$$

$$A_{M,0}e^{-\mathbf{i}\hat{k}_{M,0}\bar{x}_{M-1}} = -\frac{\mathbf{i}\bar{a}K_T e^{\mathbf{i}\theta_T}}{\sigma}\frac{1}{\cosh k_{M,0}h_M} \quad (35)$$

$$A_{1,n} = 0 \text{ for region of } n = 1,2,\dots,N \quad (36)$$

and

$$B_{M,n} = 0 \text{ for region of } n = 0,1,2,\dots,N. \quad (37)$$

By using Eq. (18), Eqs. (24) and (26) are equivalent to

$$\sum_{n=0}^{N}\begin{pmatrix}\mathbf{i}\hat{k}_{m,n}A_{m,n}\xi_{m,n}^{(1)}(x_m)\\ -\mathbf{i}\hat{k}_{m,n}B_{m,n}\xi_{m,n}^{(2)}(x_m)\end{pmatrix}\langle\zeta_{m,n}|\zeta_{m,l}^{larger}\rangle =$$
$$\sum_{n=0}^{N}\begin{pmatrix}\mathbf{i}\hat{k}_{m+1,n}A_{m+1,n}\xi_{m+1,n}^{(1)}(x_m)\\ -\mathbf{i}\hat{k}_{m+1,n}B_{m+1,n}\xi_{m,n}^{(2)}(x_m)\end{pmatrix}\langle\zeta_{m+1,n}|\zeta_{m,l}^{larger}\rangle \quad (38)$$

and

$$\sum_{n=0}^{N}\begin{pmatrix}A_{m,n}\xi_{m,n}^{(1)}(x_m)\\ +B_{m,n}\xi_{m,n}^{(2)}(x_m)\end{pmatrix}\langle\zeta_{m,l}^{smaller}|\zeta_{m,n}\rangle =$$
$$\sum_{n=0}^{N}\begin{pmatrix}A_{m+1,n}\xi_{m,n}^{(1)}(x_m)\\ +B_{m+1,n}\xi_{m,n}^{(2)}(x_m)\end{pmatrix}\langle\zeta_{m,l}^{smaller}|\zeta_{m+1,n}\rangle + \langle F|\zeta_{m,l}^{smaller}\rangle \quad (39)$$

for the indices of l=0, 1, 2, …, N, and m=0, 1, 2, …, M–1, the EMM generates a set of $2M(N+1)$ linear equations based on Eqs. (35)-(39), which are used to solve for the corresponding $2M(N+1)$ determine the $2M(N+1)$ unknown coeffcicients. The specific values of the reflection and transmission coefficients $K_R e^{\mathbf{i}\theta_R}$ and $K_T e^{\mathbf{i}\theta_T}$ are subsequently determined using Eqs. (33) and (34).

3. VALIDATIONS

In this following section, the scattered waves by permeable barriers with uniform and undulated bottom are calculated by applying the proposed EMM. To validate the accuracy of model, the results are compared with other data available in the literatures.

3.1. Oblique water waves reflected by dual thin surface-piercing barriers with stepped bottom

Firstly, the EMM is validated through the issue of the convergences of mode N. Reflection coefficients $|R|$ of water waves by dual surface piercing barriers with stepped bottom topography are calculated and compared with the results of Wang, *et al.* [24]. The dual barriers length are set as $a_1/h_1 = a_2/h_1 = 0.25$, the ratio between the deeper and shallower waters depth being $h_2/h_1 = 0.25$, the value oblique incidence wave angle $\gamma = 30°$, the ratio between water depth and wavelength $h_1/\lambda = 0.04$, with values of evanescent modes $N = 5, 25$ and 50, respectively. These are theoretical/numerical investigations on the perfomance of FPs in the coastal or shallow-to-intermediate depth regimes. In this study, the water waves can be considered as finite water depth. As illustrated in Figure 3, the variations of $|R|$ against dimensionless parameter kh_1 with values of $N = 50$ is reasonable for gaining good accordance with the findings of work [24].

3.2. Water waves reflected by uneven bottom topography

Secondly, the proposed model is applied to deal with the water wave scattering by the uneven bottom with the convergence of the shelves M. Following Porter and Porter [25], the bottom profile can be written as follows

$$h(x) = \begin{cases} h_1 & x < \bar{x}_1 \\ 1 - \alpha x^2 + (1-\alpha)x & \bar{x}_1 \le x \le \bar{x}_2 \\ h_2 & \bar{x}_2 < x \end{cases} \quad (40)$$

The sea bottom parameters are set as follows: $h_1 = 1.0m, \gamma = 0°$, the variation of bottom from $\bar{x}_1 = 0$ to $\bar{x}_2 = 0.75$, with $\alpha = 1$ presents the quadratic bottom shape. While $\alpha = 0$, the sea bottom can be considered as a flat slope bottom. Figure 4 shows the variations of |R| against dimensionless wave number kh_1 with values of M = 10, 20, and 50. As shown in the figure, $|R|$ agrees well with the literature while M increases to 50. The figure reveals that the plotted curves of $|R|$ show a close correspondence with those reported in [25] while M increases to 50. From the two examples, in this study, the validation if conducted with $N = 50$, and $M = 50$, with value of bottom parameter $\alpha = 0$.

4. DISCUSSIONS

The suggested EMM is used to study the reflection of water waves with the combined effects of surface-piercing barriers and a single triangular FP over a sloped bottom. As discussed above, in this section, the value of number of modes and shelves is taken as $N = M = 50$.

4.1. Influences of water depth

The slope of the bottom topography strongly depends on the values of right and left-hand bottom depth ratios h_2/h_1. The triangular FP parameters are set as follows: platform width $w_p/h_1 = 0.3$, platform depth $h_p/h_1 = 0.1$, located at $x_p/h_1 = 0.3$. The flat slope from $\bar{x}_1 = 0$ to $\bar{x}_2 = h_1$. Figure 5a) and b) respectively show the relationship between the $|R|$ and $|T|$ against the dimensionless wave number kh_1 with different values of bottom depth ratio h_2/h_1=0.3; 0.5; 0.7; and 0.9, respectively. As illustrated in the figure, when $kh_1 < 2$, the lower value of bottom depth ratio h_2/h_1 result in more wave reflection and reduce the transmission

coefficnet. The magnitudes of $|R|$ and $|T|$ slightly decrease and increase, respectively, when $kh_1 > 2$ with lower value in comparison with the larger value of h_2/h_1.

4.2. Influences of platform depth

Subsequently, the proposed model is employed to study the influence of triangular FP depth on the reflected water waves. The sloped bottom depth ratio $h_2/h_1 = 0.9$. The FP parameters are set as follows: $w_p/h_1 = 0.3$, located at $x_p/h_1 = 0.3$. The variations of $|R|$ and $|T|$ against dimensionless parameter kh_1 with values of platform depth $h_p/h_1 = 0.1;\ 0.2;\ 0.3, \text{and } 0.4$ are respectively shown in Figure 6a) and b). The reflection of water waves become stronger when the platform depth h_p/h_1 increase, especially with value of h_p/h_1 increase to 0.4 and higher. Beside that, the curves of $|T|$ significantly drop down when h_p/h_1 increase. When the platform draft occupies a larger portion of the water column, there is less vertical space for the oscillatory flow to pass beneath the platform, so the propagating mode beneath the structure is strongly constrained and more of the incident energy must be redirected rather than transmitted.

4.3. Influences of platform width

After that, the influences of platform width w_p/h_1 to the reflection of water waves are studied. The parameters of bottom topography are set exactly same with the previous section. The platform depth h_p/h_1 is 0.1. Figs. 7a and b respectively show the variation of $|R|$ and $|T|$ with the dimensionless wave number kh_1 with different values of bottom w_p/h_1 =0.2; 0.3; 0.4; and 0.5, respectively. It can be seen that the $|R|$ also increases with value of w_p/h_1. At lower values of kh_1, the differences among curves of $|R|$ and $|T|$ are smaller. There differences are observed that separate more distinctly while kh_1 increases. The wider platform results in stronger reflection and transmision coefficient, especially as the dimensionless wave number kh_1 increases.

4.4. Influences of barrier length

Subsequently, the proposed model is applied to study the influences of barrier lengths a_i/h_1 on the reflection of water waves. The parameters of bottom topography are set exactly same with the previous section. The platform depth and width $h_p/h_1 = 0.1,\ \ w_p/h_1 = 0.3$, respectively, located at $x_p/h_1 = 0.3$. Dual surface-piercing barriers are attached to the triangular FP, with values of barrier lengths $a_1/h_1 = a_2/h_1 = a_i/h_1$, respectively located at positions $v_1/h_1 = x_p/h_1 + 0.25w_p/h_1, v_2/h_1 = x_p/h_1 + 0.75w_p/h_1$. Figure 8a and b respectively show the variations of the $|R|$ and $|T|$ against the dimensionless wave number kh_1 with different values of barrier lengths $a_1/h_1 = a_2/h_1 = a_i/h_1$=0; 0.1; 0.2; and 0.3, where a_i/h_1=0 present the case of platform without barrier. The enhancement of $|R|$ while increasing the barrier lengths can be observed that more significant than the case of platform depth. Besides, with increasing of kh_1, $|T|$ decreases more rapidly as values of barrier lengths longer, and for the largest barrier length it tends toward zero, meaning that almost no wave energy penetrates to the lee side. This behaviour reflects both the reduced effective flow area between the longer barriers and the stronger multiple reflections and standing-wave patterns generated in the barrier region, which together trap energy and convert it into reflected waves instead of transmitted ones. The dual-barrier arrangement introduces the cavity-type resonance, so incoming energy is both intercepted at the surface and repeatedly reflected within the gap before a small remainder can leak past the system. This phenomenon could be valuable in the design, installation and operation of floating platform with thin barriers to reach higher effect and reduce construction cost.

5. CONCLUSION

This paper presented an extended EMM for analyzing the reflection of water waves by a triangular floating platform in combination with dual thin barriers over a sloped seabed. The bottom profile was discretized into a series of continuous flat shelves, and the governing conservation equations were formulated using eigenfunctions. The SuperLU sparse matrix solver was utilized to solve the resulting linear system. This solver handled the system of equations generated from the sparse matrix structure. Furthermore, the EMM approach can be simplified to model classical EMM scenarios, such as cases with an uneven seabed without barriers or a floating platform. EMM transforms complex boundary-value problems into sparse linear systems, which are efficient to solve using modern sparse-matrix solvers. For many linear problems, EMM achieves high computational efficiency. However, it is primarily restricted to linear wave theory and time-independent problems in 2D or simple 3D axisymmetric domains. It is difficult to extend to nonlinear water wave propagation or arbitrary 3D domains. Furthermore, it requires the domain to be approximated as a sequence of flat shelves or sections with abrupt change, and may create a challenge to handle complex, smoothly varying bottom topographies. After that, the validations of suggested model was examined through the problems of scattered waves by thin barriers over a step, and uneven bottom topography. Parametric investigations revealed that wave reflection is strongly influenced by the seabed configurations, platform, and barrier parameters. Notably, the incorporation of thin barriers along the platform significantly enhances wave reflection, suggesting an effective and cost-efficient strategy for optimizing the hydrodynamic performance of floating offshore platforms.

REFERENCES

[1] R. Porter and D. V. Evans, “Complementary approximations to wave scattering by vertical barriers,” *Journal of Fluid Mechanics*, vol. 294, pp. 155-180, 1995.

[2] M. A. Losada, I. J. Losada, and A. J. Roldán, “Propagation of oblique incident modulated waves past rigid, vertical thin barriers,” *Applied Ocean Research*, vol. 15, pp. 305-310, 1993.

[3] I. J. Losada, M. A. Losada, and A. Roldán, "Propagation of oblique incident waves past rigid vertical thin barriers," *Applied Ocean Research*, vol. 14, pp. 191-199, 1992.
[4] I. J. Losada, M. A. Losada, and R. Losada, "Wave spectrum scattering by vertical thin barriers," *Applied ocean research*, vol. 16, pp. 123-128, 1994.
[5] R. A. Dalrymple, M. A. Losada, and P. A. Martin, "Reflection and transmission from porous structures under oblique wave attack," *Journal of Fluid Mechanics*, vol. 224, pp. 625-644, 1991.
[6] M. M. Lee and A. T. Chwang, "Scattering and radiation of water waves by permeable barriers," *Physics of Fluids*, vol. 12, pp. 54-65, 2000.
[7] A. J. Li, Y. Liu, and H. J. Li, "Accurate solutions to water wave scattering by vertical thin porous barriers," *Mathematical Problems in Engineering*, vol. 3, pp. 985731, 2015.
[8] S. Gupta and R. Gayen, "Scattering of oblique water waves by two thin unequal barriers with non-uniform permeability," *Journal of Engineering Mathematics*, vol. 112, pp. 37-61, 2018.
[9] J. Dai et al, "Review of recent research and developments on floating breakwaters," *Ocean Engineering*, vol. 158, pp. 132-151, 2018.
[10] R. Mondal and M. M. Alam, "Water wave scattering by an array of rectangular breakwaters on a step bottom topography," *Ocean Engineering*, vol. 169, pp. 359-369, 2018.
[11] C. C. Tsai et al., "Step approximation of water wave scattering caused by tension-leg structures over uneven bottoms," *Ocean Engineering*, vol. 166, pp. 208-225, 2018.
[12] E. Masoudi and L. Gan, "Diffraction waves on general two-legged rectangular floating breakwaters," *Ocean Engineering*, vol. 235, pp. 109420, 2021.
[13] D. Paul and H. Behera, "Wave attenuation on a floating rigid dock by multiple surface-piercing vertical thin perforated barriers," *Engineering Analysis with Boundary Elements*, vol. 169, pp. 105985, 2024.
[14] C. Bi, M. S. Wu, and A. W. K. Law, "Stabilisation of compliant floating platforms with sheet barriers under wave action," *Ocean Engineering*, vol. 240, pp. 109933, 2021.
[15] J. N. Newman, "Propagation of water waves past long two-dimensional obstacles," *Journal of Fluid Mechanics*, vol. 23, pp. 23-29, 1965.
[16] J. N. Newman, "Propagation of water waves over an infinite step," *Journal of Fluid Mechanics*, vol. 23, pp. 399-415, 1965.
[17] C. C. Tsai, Y. T. Lin, and T. W. Hsu, "On the weak viscous effect of the reflection and transmission over an arbitrary topography," *Physics of Fluids*, vol. 25, pp. 043103, 2013.
[18] C. T. Tran, J. Y. Chang, and C. C. Tsai, "Step approximation for water wave scattering by multiple thin barriers over undulated bottoms," *Journal of Marine Science and Engineering*, vol. 9, pp. 629, 2021.
[19] T. J O'Hare and A. G. Davies, "A comparison of two models for surface-wave propagation over rapidly varying topography," *Applied Ocean Research*, vol. 15, pp. 1-11, 1993.
[20] T. J. O'Hare and A. Davies, "A new model for surface wave propagation over undulating topography," *Coastal Engineering*, vol. 18, pp. 251-266, 1992.
[21] S. K. Poguluri and I. H. Cho, "Analytical and numerical study of wave interaction with a vertical slotted barrier," *Ships and Offshore Structures*, vol. 16, pp. 1012-1024, 2021.
[22] P. L. F. Liu and I. J. Losada, "Wave propagation modeling in coastal engineering," *Journal of Hydraulic Research*, vol. 40, pp. 229-240, 2002.
[23] K. A. Belibassakis and G. A. Athanassoulis, "A coupled-mode system with application to nonlinear water waves propagating in finite water depth and in variable bathymetry regions," *Coastal Engineering*, vol. 58, pp. 337-350, 2011.
[24] L. X. Wang et al., "Scattering of oblique water waves by two unequal surface-piercing vertical thin plates with stepped bottom topography," *China Ocean Engineering*, vol. 32, pp. 524-535, 2018.
[25] R. Porter and D. Porter, "Water wave scattering by a step of arbitrary profile," *Journal of Fluid Mechanics*, vol. 411, pp. 131-164, 2000.